

Probabilistic Seismic Demand Assessment of Steel Moment Resisting Frames Isolated by LRB

Nader Fanaie*, Mohammad Sadegh Kolbadi** and Ebrahim Afsar Dizaj***

ARTICLE INFO

Article history:

Received:

April 2017

Revised:

June 2017

Accepted:

October 2017

Keywords:

Base isolation;

Response modification
factor;

Ductility factor;

Overstrength factor;

Fragility curve;

PSDA

Abstract:

Seismic isolation is an effective approach used in controlling the seismic responses and retrofitting of structures. The construction and installation of such systems are expanded nowadays due to modern improvements in technology. In this research, the seismic performance of steel moment resisting frames isolated by Lead Rubber Bearing (LRB) is assessed, and the seismic demand hazard curves of the frames are developed using Probabilistic Seismic Demand Analysis (PSDA). In addition, the effects of LRB on overstrength, ductility and response modification factor of the frames are studied. To achieve this, Incremental Dynamic Analyses (IDA) are conducted using 10 records of near field earthquake ground motions on the intermediate steel moment resisting fixed base frames with 3, 6 and 9 storeys retrofitted by LRB according to ASCE 41. The results show that in the case of isolated frames, the values of ductility and response modification factor are decreased in comparison with those of fixed base frames. Moreover, based on the developed fragility curves, seismic isolation is more effective in improving structural performance in extensive and complete damage states compared to slight and moderate damage states. However, increasing the height of both structural groups (i.e. fixed base and base isolated) results in reduction in performance level. Besides, the probability of occurrence of a certain demand is reduced by base isolation.

1. Introduction

Seismic performance evaluation of structures is of significant importance taking into consideration the modern philosophy of design. In addition to the uncertainties, seismic demand and structural capacity should also be considered in evaluating the seismic performance of structures. Almost all the researches in the field of seismic base isolation have shown that seismic protection is extremely effective in minimizing the damage of certain types of buildings during seismic action.

The ordinary methods of seismic design are based on increasing the capacity of structures. Increasing the stiffness of structures results in more absorption of earthquake loads. However, seismic isolator systems isolate the structures from the ground and provide the needed flexibility by concentrating on the displacements that occur in the isolated level. Under such conditions, a system is created with a much lower frequency than the dominant frequency of the earthquake. Seismic base isolators improve the seismic performance of structures by increasing their periods and decreasing their seismic demands (Naeim *et al.*, 1999[21]). Therefore, using fragility curves to assess the seismic performance of isolated structures is an appropriate and reliable approach to select the best option in retrofitting the structures and managing the earthquake risk. It should be mentioned that ductility plays an effective role in the response modification factor and seismic performance of the structures. Due to the lack of information on the philosophy

* Corresponding author: Associate Professor, K. N. Toosi University of Technology, Civil Engineering Department, Tehran, Iran, E-mail address: fanaie@kntu.ac.ir

** Graduated Student in Earthquake Engineering, Department of Civil Engineering, Isfahan (khorasgan) Branch, Islamic Azad University, Isfahan, Iran,

*** Ph.D of Structural Engineering, Faculty of Engineering, University of Guilan, Rasht, Iran,

of the suggested response modification factor of isolated buildings in seismic rehabilitation codes, this factor is calculated for these specific systems in this study. To the authors' knowledge, this is the earliest study executed to investigate the ductility, overstrength and response modification factor of isolated structures and compare them with the values suggested by seismic rehabilitation codes.

So far, different practical and theoretical researches have been conducted on the seismic performance of structures equipped with base isolators. Tena-Colunga & Gómez-Soberón (2002) [27] compared the displacement response amplifications of the base isolation system of an asymmetric structure with the response of a symmetric structure. It was shown that base displacement demand amplifications are higher for larger eccentricities of superstructures, and they depend on the periods of isolated structures. Based on their conclusions, asymmetry reduces the effectiveness of base isolation systems, since more exposed isolators tend to deform plastically, while others still remain elastic. Moreover, contrary to expectations, maximum base displacement is recorded for unidirectional eccentricity instead of bidirectional eccentricity. Karim & Yamazki (2007)[14] investigated the effects of using base isolators on the fragility curves in highway bridges and suggested a simple method of deriving the mentioned curves. They modelled 30 bridges, with different heights, weights and overstrength factors, subjected to 250 earthquake records. They used PGA and PGV as Intensity Measure (IM) in their research. Comparing the curves plotted for isolated and fixed base structures, they concluded that isolation increased fragility in tall pier bridges compared to short pier ones. They designed a type of isolator for all pier heights; however, they did not consider the effect of isolator damage. Han *et al* (2014) [10] has used the seismic risk analysis for an old non-ductile RC frame building before and after retrofit with base isolation. The study revealed that base isolation can greatly reduce the seismic risk for higher damage levels, as expected. More importantly, the results also indicated that neglecting aftershocks can cause considerable underestimation of the seismic risk. Dezfuli *et al* (2018) [8] developed a new constitutive material model for SMA-LRB. The outcome of their study shows that SMA wires can efficiently reduce the shear strain demand in LRBs. Nakhostin Faal and Poursha (2017) [23] successfully extended the modal pushover analysis and N_2 method to account for higher mode effects on seismic behavior of LRB buildings.

This research investigates the effects of seismic isolation with LRB on steel structures using IDA curves. For this purpose, incremental dynamic analysis is conducted on each considered model by 10 near field earthquake records using OpenSees software. The probability that the structural system will fail to meet the desired performance is evaluated

through Limit State (LS) analysis of IDA data, i.e., conditional probability of exceedance as a function of S_a values is generated for the considered LS's. The resulting curves, known as fragility curves, are used in the next step to tabulate the capacities of structures in terms of S_a values corresponding to different failure probabilities, regarding various performance levels (i.e. LS's). In addition to limit state conditions, the Probabilistic Seismic Demand Analysis (PSDA) (Cornell 1996[5]; Jalali *et al* 2012[12]) framework is applied to calculate the Mean Annual Frequency (MAF) of LS exceedance for multiple demand levels. The results are presented as the "seismic demand hazard curves" of structures (Jalali *et al* 2012[13]; Shome & Cornell 1999[25]).

2. LRB seismic isolator system

LRB isolators are similar to the rubber ones with low damping except that they have one or more lead bearings, as shown in Fig.1. The mentioned lead bearings are physically deformed under about 10 MPa shearing stress, causing the creation of a bi-linear response in the bearing (Tyler & Robinson 1984[28]). Rubber bearing with lead core is a nonlinear system modelled based on the bi-linear force-displacement curve presented in Fig.2. In Fig.2, Q_d is the specified strength which can be equal to the yielding force of the lead core; K_{eff} is the effective stiffness of LRB in the horizontal displacement (D), which is higher than the yielding displacement (D_y); K_I and K_p are the stiffness values before and after yielding, respectively. The ratio of K_p to K_I is considered as 0.1 (ASCE 2013[3]). The damping response factor (β_m) is considered as 1.38 for 15% damping based on the ASCE7 guideline (2010)[2].

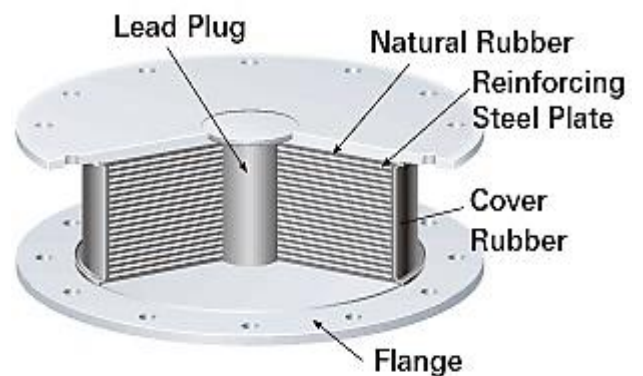


Fig. 1: Lead-rubber bearing (Naeim & Kelly 1999[21])

3. The studied models

In this research, 3-, 6- and 9-storey structures with storey height of 3.2m and lateral loading system of intermediate steel moment resisting frames are designed according to ASCE7 guideline (2010)[2] and AISC (2010)[1] codes.

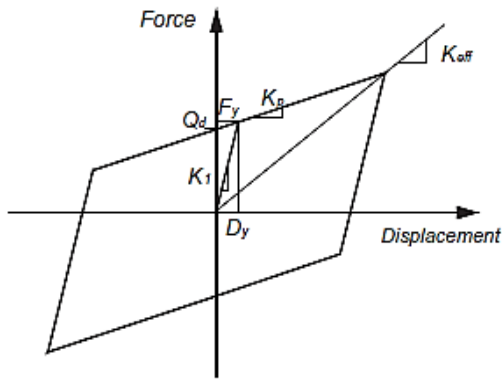


Fig. 2: Idealized hysteretic force-displacement relation of a lead-rubber bearing (Han *et al* 2014[10])

It is assumed that the structures are constructed in a region with high seismicity on soil type II, based on the Iranian Seismic Code (2005)[5]; with an average shear wave velocity of 360-750 m/s² in a depth of 30 m. The steel used is ST-37 and the span length is 4m. The plans of all storeys are considered the same in the studied structures and are presented in Fig.3 (a). The configurations of the frames derived from 3-D structures (frame A in Fig.3 (a)) are shown in Fig.3 (b).

4. Modelling of LRB isolator

In this study, the isolators are designed for the most powerful considered earthquake (BSE-2X) according to the seismic rehabilitation code of ASCE 2013[3], using Eqs. (1) to (6). The wind load on the isolated building is also checked to ensure that the LRBs will not yield under wind action. The specifications of the designed isolators are presented in Table 1.

$$K_{eff} = \frac{W}{g} \left(\frac{2\pi}{T_M} \right)^2 \quad (1)$$

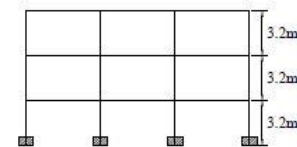
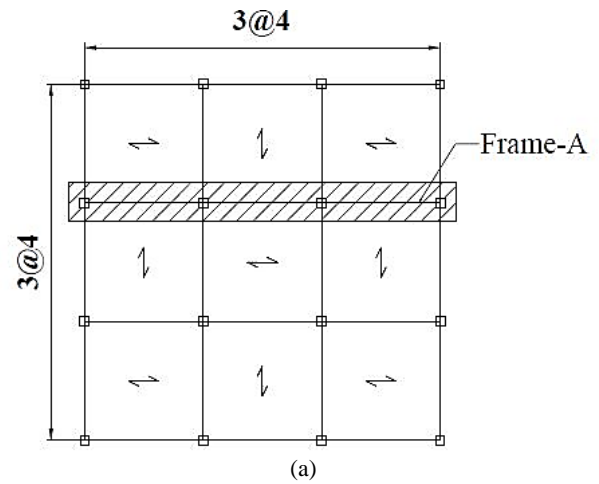
$$D_M = \left[\frac{g}{4\pi^2} \right] \frac{S_{x1}}{B_M} T_M \quad (2)$$

$$Q = \frac{\pi \times K_{eff} \beta_{eff} \times (D)^2}{4(D - D_y)} \quad (3)$$

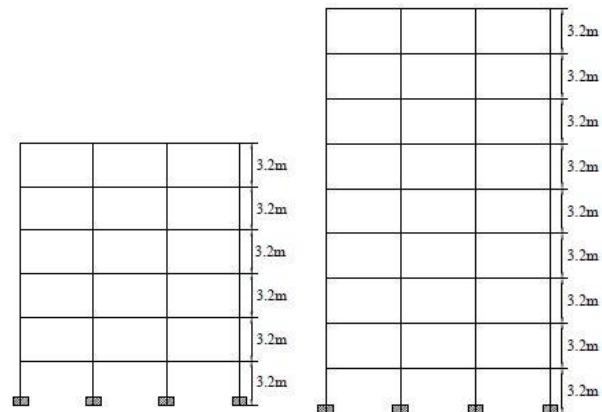
$$K_e = K_{eff} - \frac{Q}{D_M} \quad (4)$$

$$D'_M = \frac{D_M}{\sqrt{1 + \left[\frac{T_e}{T_M} \right]^2}} \quad (5)$$

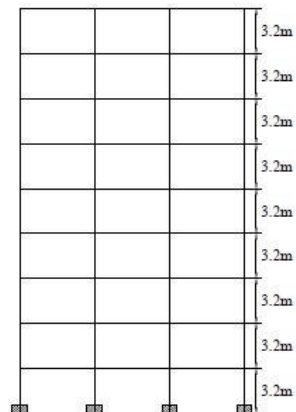
$$T_M = 2\pi \sqrt{\frac{W}{g \times K_M}} \quad (6)$$



(b)



(c)



(d)

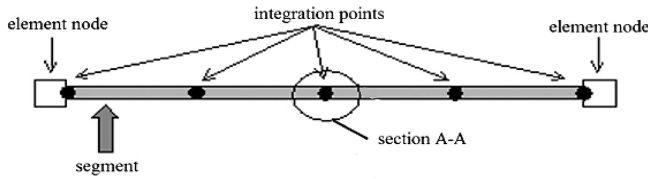
Fig. 3: 2D studied models: (a) Plan of the studied models, (b) 3-storey frame, (c) 6-storey frame and (d) 9-storey frame

where g is acceleration due to gravity; W is the effective seismic weight; Q is the characteristic strength; T_M is the effective period of the isolated building at the maximum displacement of the BSE-2X; D_M is the maximum displacement of the isolation system; D'_M is the target displacement of the BSE-2X; S_{x1} is the spectral response acceleration parameter at 1.0 s, which is evaluated for the BSE-2X; T_e is the effective period of the structure above the isolation interface on a fixed base; K_M is the effective stiffness of the isolation system at the design displacement in the horizontal direction under consideration.

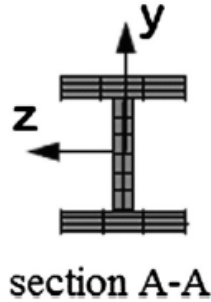
Table 1: Specifications of designed isolators

No.Story	T _D (m)	D _D (m)	D' _D (m)	K _e (kN/m)	K _P (kN/m)	K _{eff} (kN/m)	Q _d (kN)
3	2.00	0.24	0.22	198.81	19.88	26.00	1.48
6	2.50	0.23	0.21	258.00	25.80	33.75	1.87
9	3.00	0.28	0.27	271.70	27.17	35.55	2.37

In order to conduct nonlinear analysis, OpenSees software is used. It is a finite element method based on object-oriented framework for simulating the seismic response of structural systems. Nonlinear beam-column element is employed to model the beam and column elements in the nonlinear range of deformation in this software. This element can take the effects of P-Δ and large deformations into account when considering the geometrical nonlinear effects of the model. In order to model wide plasticity in the member length, each element, including the beam and column, is divided into several fibers along its section and several segments along its length (Fig. 4 (a) and (b)) (Mazzoni *et al* 2007[19]). The LRBs are simulated using the zero length section element with the Isolator2spring section, which was developed by Ryan *et al* (2005) [29].



(a)Dividing the element into several segments



(b)Dividing the section into fibers

Fig. 4: Schematic division of element and section into segment and fiber elements in OpenSees (Mazzoni *et al* 2007[18])

5. Basis of calculating Response modification factor

In this research, the method presented in Uang (1991) [30] is used to calculate response modification factor. Fig.5 shows the nonlinear behaviour of the structure. According to Fig.5, maximum base shear (V_e) is reduced to yielding force

(V_y) due to the ductility and nonlinear behaviour of the structure. The force reduction factor due to ductility, overstrength and response modification factor are respectively defined as follows (Uang 1991[29]; Fanaie & Ezzatshoar 2014 [9]):

$$R_\mu = V_e / V_y \quad (7)$$

$$R_s = V_y / V_s \quad (8)$$

$$R = (V_e / V_s) = (V_e / V_y) \times (V_y / V_s) = R_\mu \times R_s \quad (9)$$

$$R = (V_e / V_w) = (V_e / V_y) \times (V_y / V_s) \times (V_s / V_w) = R_\mu \times R_s \times \gamma \quad (10)$$

Where V_y is the base shear corresponding to mechanism formation; V_s is the base shear of the first plastic hinge formation. Eqs 9 and 10 present the response modification factor based on ultimate strength and allowable stress design methods, respectively. According to the design codes in the allowable stress design method γ is an allowable stress factor, defined according to Eq. (11). In this study, γ is taken as 1.44 based on the recommendations of UBC-97 (Uang (1991) [30]; Fanaie & Ezzatshoar 2014 [9]).

$$\gamma = V_s / V_w \quad (11)$$

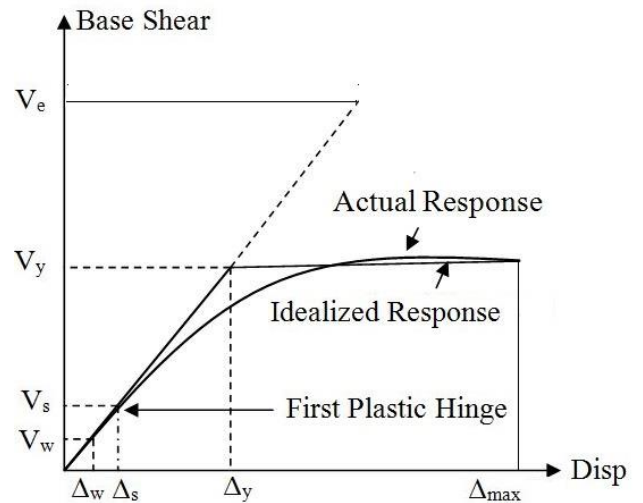


Fig. 5: Nonlinear behavior of structure [6]

6. Calculating the response modification factor using IDA

6.1 Overstrength factor (R_s)

Mwafy and Elnashai (2002) [20] have provided a method to obtain maximum base shear using nonlinear dynamic analysis. Overstrength factor (R_s) is computed according to Eq. (12) and modified based on the results of Massumi and Tasnimi (2004) [18].

$$R_s = V_{b(Dyn,y)} / V_{b(st,s)} \quad (12)$$

Where $V_{b(Dyn,y)}$ is dynamic base shear, and $V_{b(st,s)}$ is static base shear corresponding to the first yielding point of the structure.

6.2 Ductility factor (R_μ)

Ductility factor is the ratio of the maximum linear base shear ($V_{b(Dyn,e)}$) to the maximum nonlinear base shear of the structure ($V_{b(Dyn,y)}$); both correspond to the target limit state and are obtained by IDA under the same records (Fanaie & Ezzatshoar 2014 [9]).

$$R_\mu = V_{b(Dyn,e)} / V_{b(Dyn,y)} \quad (13)$$

7. Incremental dynamic analysis (IDA)

IDA is a nonlinear dynamic analysis through which the damage level can be identified as per the intensity of the applied earthquake. The intensity of ground motion measured by IM, incrementally increases in each analysis. Drift ratio, an engineering demand parameter (EDP), is monitored during each analysis. The extreme values of the EDP are plotted against the corresponding values of ground motion IM for each intensity level to derive a dynamic pushover curve for the structure and chosen earthquake record. This method is also used to consider the effects of aleatory uncertainty existing in the earthquakes on the evaluation of seismic responses of structures. Therefore, an appropriate number of earthquake records should be applied to consider the uncertainty existing in their frequency content. A sample of IDA curves is presented in Fig. 6.

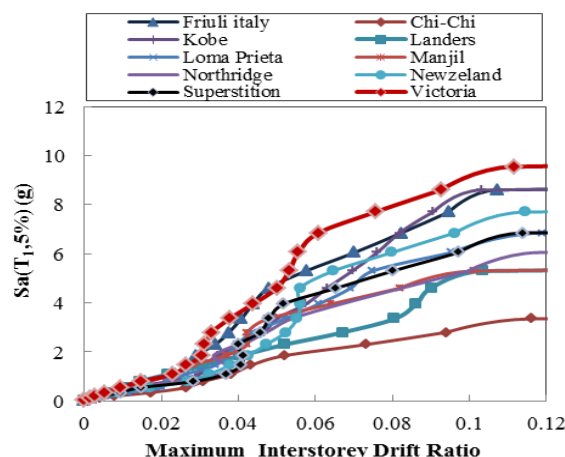


Fig. 6: IDA curves for 9-storey fixed base frame

7.1 Limit state

FEMA, rehabilitation standards and some other codes have suggested various criteria for damage definition in different limit states. HAZUS-MH (2009) [11] suggested four damage states namely; slight, moderate, extensive and complete damages for general building. According to HAZUS-MH (2009) [11], limit states are defined based on height and lateral load resisting system for each damage state. The models studied in this research are S1 and are designed in high code seismic design level, based on HAZUS (2009) [11] categorization. It should be noted that the peak inter storey drift ratio is selected as the limit state in this study. Table 2 presents the inter-storey drift performance level of the studied models at each damage state.

7.2 Earthquake ground motions

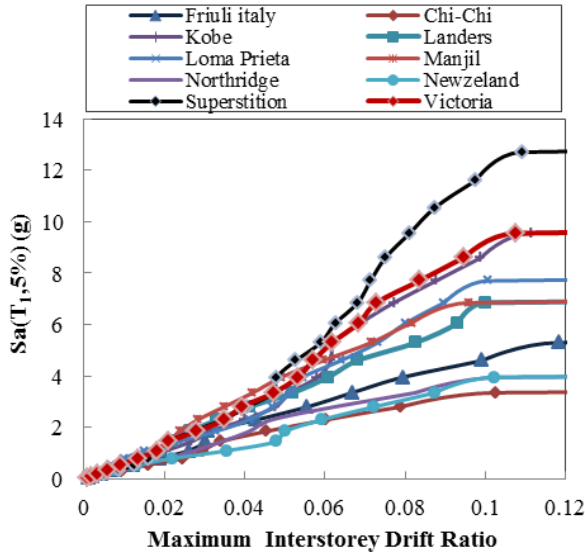
A proper number of earthquake records should be selected to determine the loading capacity of a structure up to collapse, and nonlinear time history analysis should be performed. These records should demonstrate the seismicity of the site of the considered structure as well as the seismicity level in which the design or evaluation of the structure is performed. On the other hand, the conditions of the site and type of soil have significant effects on the frequency content of earthquake records (Stewart *et al* 2002) [26]). The records considered in this research are adopted from NEHRP site class C records based on the soil type of the site of the structure. The specifications of the mentioned records are presented in Table 3. Fig.7 presents the results obtained from incremental dynamic analysis (IDA) for all fixed base and base isolated frames. In this research, FB and BI refer to fixed base and base isolated structures, respectively.

Table 2: Inter-storey drift ratio for each damage state

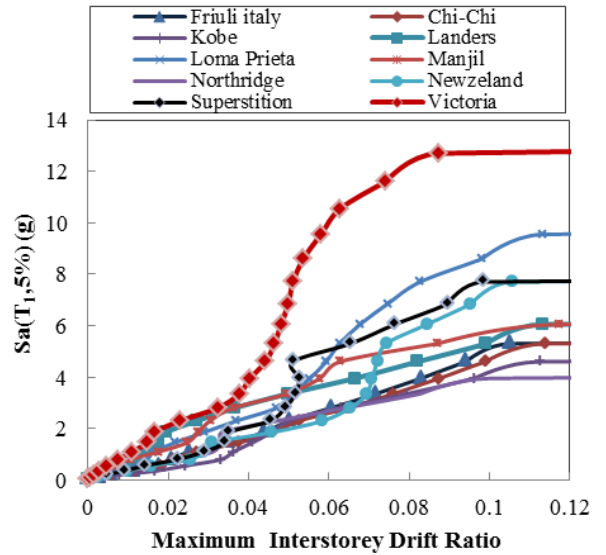
No.Storey	Building properties		Inter storey drift ratio			
	type	Height	Slight	Moderate	Extensive	Complete
3-storey	S1L	Low- Rise	0.006	0.012	0.030	0.080
6-storey	S1M	Mid-Rise	0.004	0.008	0.020	0.053
9-storey	S1H	High-Rise	0.003	0.006	0.015	0.040

Table 3: The specifications of earthquake records selected for incremental dynamic analysis

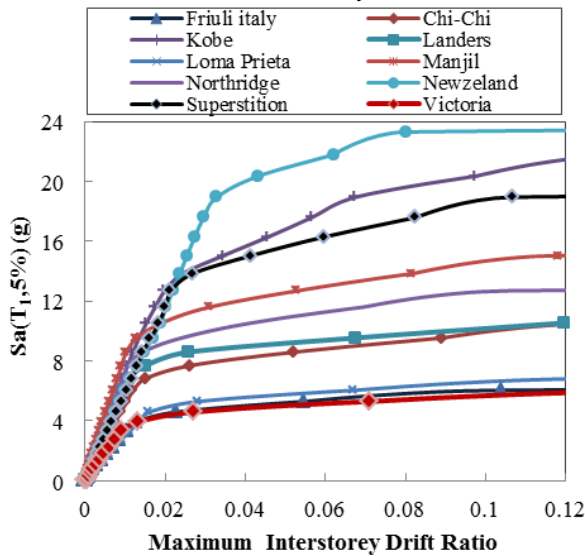
Record	Station	Earthquake Date	PGA(g)	Magnitude
Chi-Chi Taiwan-03	CWB99999TCU 129	20/09/1999	0.608	6.20
Loma Prieta	UCSC 14 WAHO	18/10/1989	0.517	6.93
Superstition Hills-02	USGS 286 Superstition Mtn Camera	24/11/1987	0.793	6.54
Friuli, Italy-01	SO12 Tolmezzo	05/06/1976	0.346	6.50
Victoria, Mexico	UNAMUCSD 6604 Cerro Prieto	06/09/1980	0.572	6.33
New Zealand-02	99999 Matahina Dam	03/02/1987	0.293	6.60
Northridge-01	USC 90014 Beverly Hills-12520 Mulhol	17/01/1994	0.510	6.69
Landers	CDMG 22170 Joshua Tree	28/06/1992	0.249	7.28
Kobe, Japan	CUE99999 Nishi-Akashi	16/01/1995	0.486	6.90
Manjil, Iran	BHRC 99999 Abbar	20/06/1990	0.505	7.37



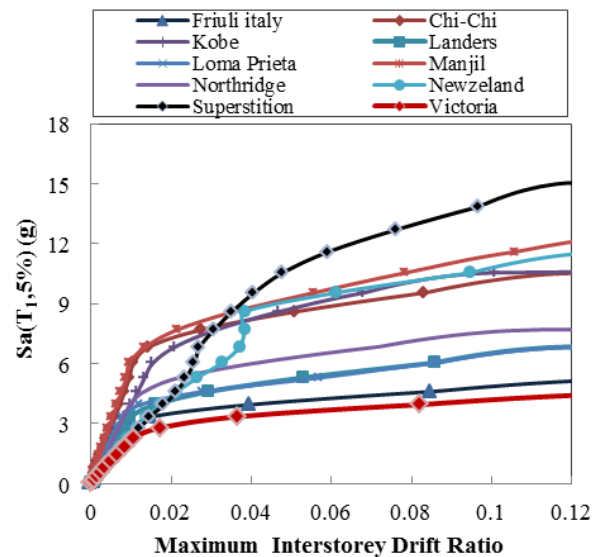
(a) 3 storey-FB



(c) 6 storey-FB



(b) 3 story-BI



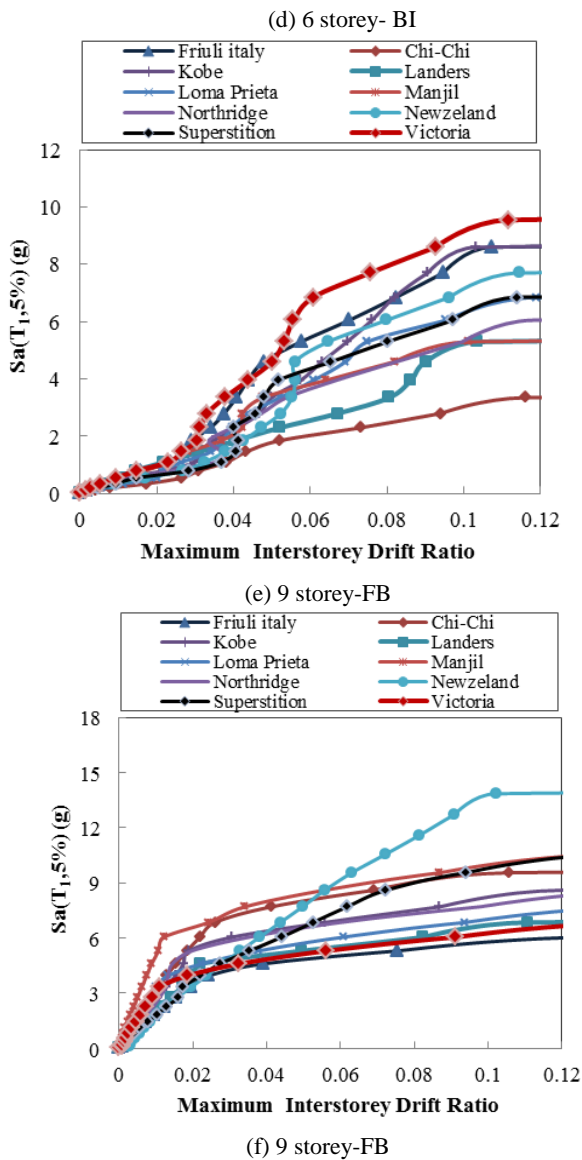


Fig. 7: IDA curves for all frames before and after retrofitting by LRB

Fig. 8 compares the median IDA curves of all the considered frames. As can be seen in Fig. 8, for different storeys, the capacity of the base isolated frames are significantly more than that of fixed-based frames.

Table 4: Sa values corresponding to different failure probabilities

No.Storey	Failure Probability	Base Isolated building				Fixed Base Buildings			
		Slight	Moderate	Extensive	Complete	Slight	Moderate	Extensive	Complete
3-storey	16%	1.97	3.91	5.49	6.75	0.22	0.45	1.74	4.24
	50%	3.91	3.91	8.63	10.64	0.28	0.58	2.22	6.19
	84%	3.78	3.91	13.56	16.76	0.38	0.74	2.85	9.03
6-storey	16%	0.74	1.60	3.00	4.24	0.04	0.12	0.38	1.58
	50%	1.08	2.29	4.12	6.00	0.11	0.22	0.66	2.64
	84%	1.57	3.28	5.66	8.49	0.19	0.38	1.15	4.43
9-storey	16%	0.31	0.8	2.27	4.29	0.02	0.11	0.28	1.17
	50%	0.52	1.21	3.07	5.17	0.06	0.16	0.39	1.66
	84%	0.88	1.81	1.57	6.23	0.12	0.22	0.53	2.34

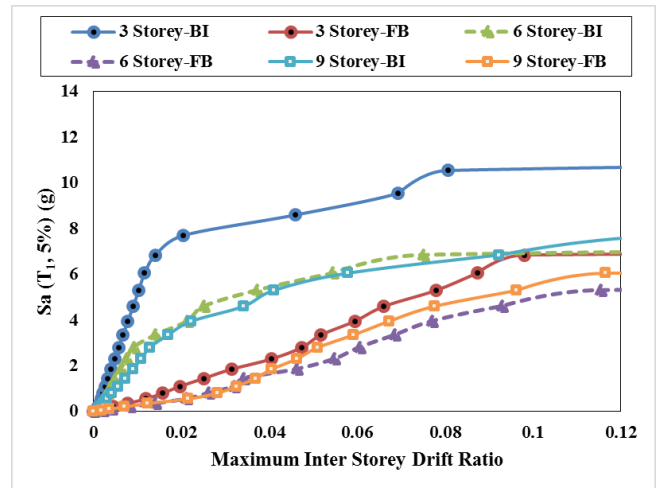


Fig. 8: Comparing median IDA curves of all the considered frames

Table 4 presents the values of Sa corresponding to 16%, 50% and 84% of structural failures for slight, moderate, extensive and complete damage states.

According to Table 4, the capacity of the structures will increase with seismic isolation. The mentioned capacity is reduced with increasing height of the structures. The values given in Table 4 can be used to identify the design earthquakes with certain probability of collapse and evaluate the capability of codes presented for designing the structures against earthquakes.

8. Non-linear static analysis (pushover)

Pushover analysis is conducted to find the values of static base shear corresponding to the first plastic hinge formation in the structures. The obtained results are tabulated in Table 5.

Table 5: First hinge base shear of models

No. Storey	Vs(ton)	
	FB	BI
3-Storey	86.27	70.43
6-Storey	52.42	73.44
9-Storey	13.47	45.56

9. Calculating response modification factor (R)

Response modification factor is calculated according to the concepts described in this study. Table 6 presents the values of overstrength, ductility and response modification factor of fixed base and base isolated models.

Table 6. Overstrength, ductility and response modification factors of all studied models

No. Storey	Type	R _S	R _μ	R _{LRFD}	R _{ASD}
3-Storey	Fixed Base Frames	2.11	2.19	4.64	6.68
6-Storey		1.99	2.21	4.31	6.21
9-Storey		1.95	2.17	4.14	5.97
3-Storey	Base Isolated Frames	1.42	1.02	1.45	2.09
6-Storey		1.34	1.05	1.41	2.04
9-Storey		1.30	1.06	1.38	1.98

10. Fragility curves

The probability of exceeding a certain level or occurrence of damage can be expressed by the specifications of earthquake such as PGA, PGV and spectral acceleration corresponding to the first mode of the structure ($Sa(T_1)$). The values are usually calculated for different structural and non-structural components sensitive to the relative displacement, and non-structural components sensitive to the acceleration, to quantitatively express the vulnerability of different structural and/or non-structural components as per the seismic risk level. However, it should be noted that this research mainly focuses on the structural elements. The normalized curves, called fragility curves, are plotted by repeating the operations for different values of $Sa(T_1)$ or other similar parameters. Researchers have suggested different numerical scales for earthquake intensity such as PGA, PGV and $Sa(T_1)$ (Cordova et al 2001[6]; Hutchinson et al 2004[12]). $Sa(T_1)$ is the most ordinary selected scale for the intensity of earthquake compared to other scales, such as peak ground acceleration (PGA) which is independent of the structure (Shome et al 1998[24]; Luco & Cornell 2007[16]). Fragility curves are generally plotted by lognormal cumulative distribution function (Aslani 2005[4]; Wen and Ellingwood 2005[31]). This research expresses the fragility curves by means of lognormal distribution function with two parameters as follows:

$$P(DS \geq ds_i | Sa(T_1)) = \Phi\left(\frac{\ln X - \mu_{ln}}{\sigma_{ln}}\right) \quad (14)$$

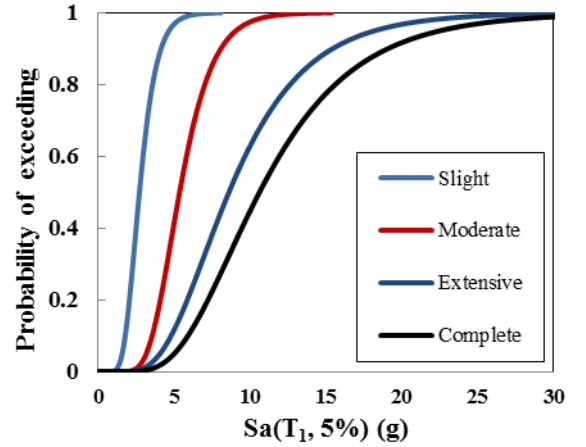
Where $P(DS \geq ds_i | Sa(T_1))$ is the probability of experiencing or exceeding damage state i ; Φ is the cumulative standard normal distribution; X is lognormal distributed spectral acceleration; and μ_{ln} is the mean variable natural logarithm given by:

$$\mu_{ln} = \ln(m) - \frac{\sigma_{ln}^2}{2} \quad (15)$$

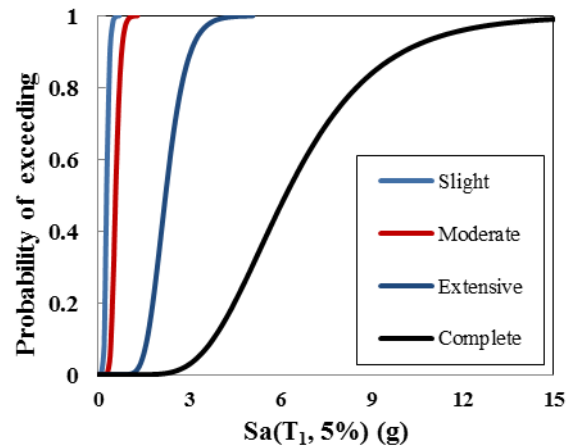
Where m is the mean non-logarithmic variables and σ_{ln} is the standard deviation of variable natural logarithm given by:

$$\sigma_{ln} = \sqrt{\ln\left(1 + \frac{S^2}{m^2}\right)} \quad (16)$$

Where S is the standard deviation of non-logarithmic variables. This research selected the earthquake intensity scale as elastic spectral acceleration with 5% damping in the main period of the structure ($Sa(T_1)$). The fragility curves are plotted for the structures after retrofitting by seismic isolator for slight, moderate, extensive and complete damage states in Fig. 9. The fragility curves of all fixed base and base isolated models are presented in Fig. 10.



(a) 3-storey



(b) 6-storey

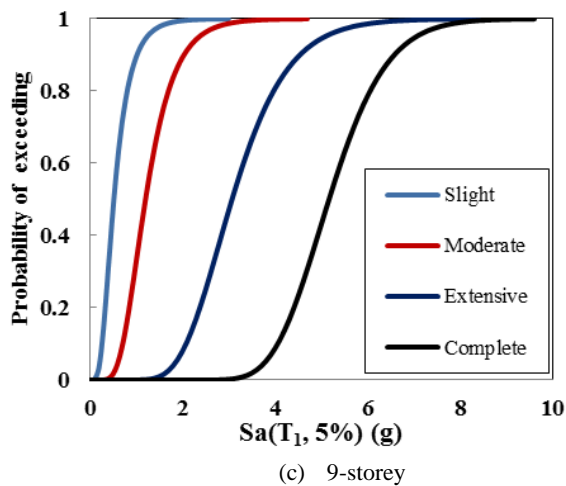


Fig. 9: Fragility curves of structures after seismic isolation for all damage states

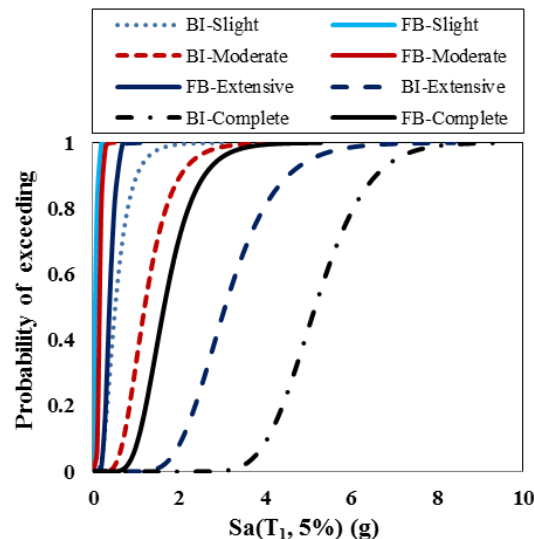
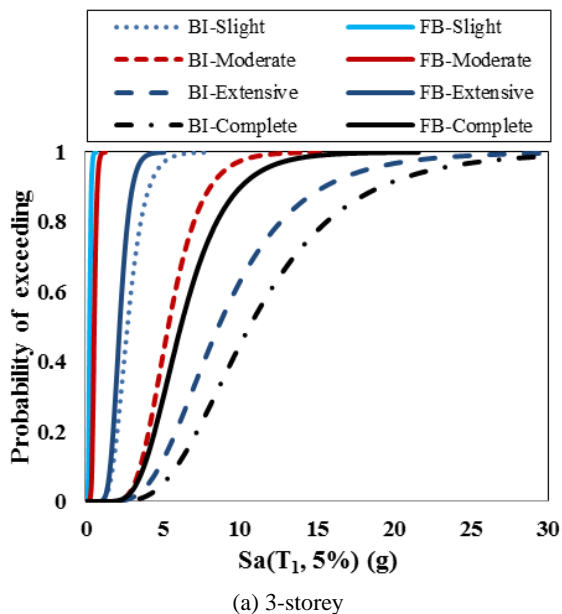
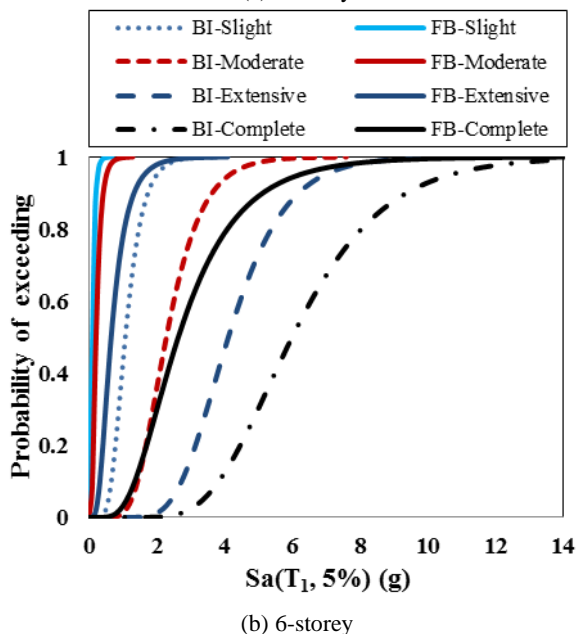


Fig. 10: Fragility curves of structures before and after seismic isolation at slight, moderate, extensive and complete performance levels



(a) 3-storey



(b) 6-storey

In general, as the heights of both fixed base and base isolated structures increase, the probability of damage occurrence increases. However, the probability of damage occurrence is less in all damage states in the isolated frames in comparison with the fixed base models. Based on Figs. 9 and 10, it can be concluded that base isolation increases structural capacity in all damage states. However, the efficiency of the base isolator system is reduced with increasing height of the structure.

11. Probabilistic Seismic Demand Analysis, PSDA

Probabilistic seismic demand analysis (PSDA) is an approach for computing the mean annual frequency of exceeding a specified seismic demand for a given structure at a designated site (Luco *et al* 2002[17]). Seismic demand hazard curve is plotted using earthquake return period and spectral acceleration in the main period of the structure ($Sa(T_1)$). This curve presents the average distribution of annual exceedance (λ) of any value of earthquake intensity scale. Seismic demand hazard curve is defined in linear form in the logarithmic scale for different selected scales of earthquake and expressed as follows (Sewell *et al* 1991[22]; Khaloo & Tonekaboni 2013[15]):

$$\lambda_{Sa(T_1)}(Sa) = k_0 (Sa)^{-k} \tag{17}$$

Where $\lambda_{Sa(T_1)}(Sa)$ is the average annual distribution of $Sa(T_1)$ exceeding Sa , and k_0 and k are the constant parameters obtained from linear regression in the logarithmic scale. Figs. 11 and 12 presents the seismic demand hazard curves of the structures before and after seismic isolation.

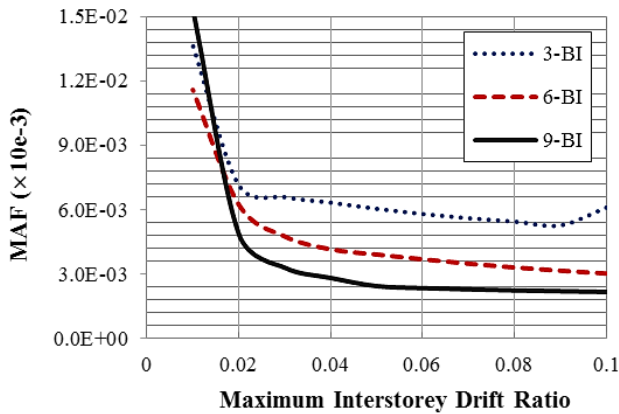


Fig. 11: Seismic demand hazard curves of the structures after seismic isolation

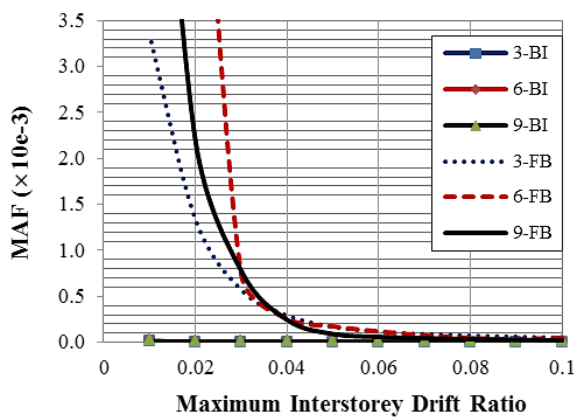


Fig. 12: Seismic demand hazard curves of the isolated and non-isolated structures

Seismic isolation reduces the probability of occurrence of a certain demand at a specific risk level. However, concerning the seismic hazard curve, the general probability of occurrence of a certain demand is reduced in both the fixed base and base isolated structures with increasing heights.

11. Conclusions

In this study, the effects of seismic isolation by lead rubber bearing on the seismic behaviour of steel moment resisting frames is investigated. To this end, the overstrength, ductility and response modification factors of the isolated structures were calculated and compared with those of fixed base structures. Moreover, the effect of base isolation on the seismic performance of steel moment resisting frames was studied using probabilistic seismic demand analysis. Finally, fragility and seismic demand hazard curves were plotted for fixed base and base isolated frames. The obtained results are briefly summarized as follows:

- The overstrength, ductility and response modification factors of structures decrease in isolated frames. The

obtained ductility factor is about 1, and the response modification factor is about 2, which are both in agreement with the values suggested in the seismic rehabilitation codes for isolated structures. In general, seismic isolation by lead rubber bearing increases the capacity of the structure and decreases the demand ductility.

- The considered fixed-based frames meet the same seismic demand levels in a lower spectral acceleration compared to the isolated ones. This increasing trend is reduced with increasing height of structures. It seems that base isolation is not an appropriate approach for improving the seismic performance of high buildings.
- The values of S_a corresponding to 50% of structural failures for all damage states show that the seismic demand of a structure is reduced or removed by seismic isolation through increasing their capacities without increasing the dimensions of sections and using lateral braces. Increasing the stiffness and providing lateral strength results in high cost of retrofitting, the effects of which dramatically deteriorate the architecture of the structure. Moreover, after seismic isolation, due to the increase in structural capacity, the probability of collapse or not meeting slight, moderate, extensive and complete performance levels are significantly reduced at a constant level of seismic intensity. Besides, the efficiency of seismic isolation in complete damage state is higher in comparison with that of other states.
- Comparing the fragility curves, the probability of exceedance of the structure from limit states is reduced by seismic isolation. However, the probability of collapse is reduced in high buildings by combining fragility curves and seismic hazard curves before and after seismic isolation. This is due to the reduction in the annual frequency of occurrence of different seismic intensities with increasing height of structures, consequently increasing its natural periods.

References

- [1] American institute of steel construction, "AISC-360-Specification for structural steel buildings", Chicago, Illinois, 2010.
- [2] American Society of Civil Engineers, "ASCE/SEI7-Minimum design loads for buildings and other structures", Reston, Virginia, 2010.
- [3] American Society of Civil Engineers, "ASCE-41-Seismic evaluation and retrofit of existing buildings", Federal Emergency Management Agency, 2013.
- [4] Aslani, H., "Probabilistic Earthquake Loss Estimation and Loss Disaggregation in Buildings", PhD Thesis, Department of Civil and Environmental Engineering, Stanford University, Stanford, CA, 2005.
- [5] BHRC, Iranian code of practice for seismic resistance design of buildings, standard No. 2800-5, 3rd edition. Building and Housing Research Center. Tehran, 2005.
- [6] Cordova, P.P., Deierlein, G.G., Mehanny, S.S.F., Cornell,

- C.A., "Development of two-parameter seismic intensity measure and probabilistic assessment procedure", Proceedings of the 2nd U.S. – Japan Workshop on Performance-based Earthquake Engineering Methodology for Reinforced Concrete Building Structures, Sapporo, Japan, 2001, p. 187–206.
- [7] Cornell, C.A., "Calculating building seismic performance reliability", Eleventh Conference on Earthquake Engineering, Acapulco, Mexico, 1996.
- [8] Dezfuli, F. H., Li, Sh., Alam, M. S., Wang, J. "Effect of constitutive models on the seismic response of an SMA-LRB isolated highway bridge", *Engineering Structures*, 2017, 148: 113–125.
- [9] Fanaie, N., Ezzatshoar, S., "Studying the seismic behavior of gate braced frames by incremental dynamic analysis (IDA)", *Constructional and steel research*, vol.99, 2014, p. 111-120.
- [10] Han, R., Li, Y., van de Lindt, J., "Seismic risk of base isolated non-ductile reinforced concrete buildings considering uncertainties and mainshock–aftershock sequences", *Structural Safety*, vol.50, 2014, p. 39-56.
- [11] HAZUS_MH MR4, Earthquake Model Technical Manual. Federal Emergency Management Agency. Washington, DC, 2009.
- [12] Hutchinson, T.C., Chai, Y.H., Boulanger, R.W., Idriss, I.M., "Inelastic seismic response of extended pile-shaft-supported bridge structures", *Earthquake Spectra*, vol.20 (4), 2004, p. 1057-1080.
- [13] Jalali, S.A., Banazadeha, M., Abolmaali, A., Tafakori, E., "Probabilistic seismic demand assessment of steel moment frames with side-plate connections", *Scientia Iranica*, vol.19 (1), 2012, 27–40.
- [14] Karim, K.R., Yamazaki, F., "Effect of isolation on fragility curves of highway bridges based on simplified approach", *Soil Dynamics and Earthquake Engineering*, vol.27 (5), 2007, p. 414–426.
- [15] Khaloo, A.R., Tonekaboni, M. "Risk based seismic assessment of structures", *Advances in Structural Engineering*, 16(2), 2013, p. 307-314.
- [16] Luco, N., Cornell, C.A., "Structure-specific scalar intensity measures for near-source and ordinary earthquake ground motions", *Earthquake Spectra*, vol. 23(3), 2007, p. 357-392.
- [17] Luco, N., Mai, P.M., Cornell, C.A., Beroza, G. C., "Probabilistic seismic demand analysis at a near fault site using ground motion simulations based on a stochastic kinematic earthquake source model", Proceedings of the 7th U.S. National Conference on Earthquake Engineering, Boston, Massachusetts 2002.
- [18] Massumi, A., Tasnimi, A.A., Saatcioglu, M., "Prediction of seismic overstrength in concrete moment resisting frames using incremental static and dynamic analysis", Proceedings of the 13th World Conference on Earthquake Engineering, Vancouver, B.C, Canada, 2004.
- [19] Mazzoni, S., McKenna, F., Scott, M.H., Fenves, G.L., Jeremic, B., "OpenSees Command Language Manual", Berkely, CA: Pacific Earthquake Engineering Center, Univ, California at Berkely, 2007.
- [20] Mwafy, A.M., Elnashai, A.S., "Calibration of force reduction factors of RC buildings", *Journal of Earthquake Engineering*, vol. 6(2), 2002: 239–73.
- [21] Naeim, F., Kelly, J.M., "Design of Seismic Isolated Structures from Theory to Practice", (6th edition), John Wiley & Sons, Inc, New York, USA, 1999.
- [22] Sewell, R.T., Toro, G.R., McGuire, R.K., "Impact of Ground Motion Characterization on Conservatism and Variability in Seismic Risk Estimates", Report NUREG/CR-6467, U.S. Nuclear Regulatory Commission, Washington, D.C, 1991.
- [23] Nakhostin Faal, H., Poursha, M. "Applicability of the N2, extended N2 and modal pushover analysis methods for the seismic evaluation of base-isolated building frames with lead rubber bearings (LRBs).", *Soil Dynamics and Earthquake Engineering*, 2017, 98: 84–100
- [24] Shome, N., Cornell, C.A., Bazzurro, P., Eduardo, C.J., "Earthquakes, records and nonlinear responses", *Earthquake Spectra*, vol.14 (3), 1998: 469–500.
- [25] Shome, N., Cornell, C.A. "Probabilistic Seismic Demand Analysis of Nonlinear Structures", RMS Report-35, Reliability of Marine Structures Group, Stanford University, Stanford, 1999.
- [26] Stewart, J.P., Chiou, S.J., Bray, J.D., Garves, R.W., Somerville, P.G., Abrahamson, N.A., "Ground motion evaluation procedures for performance based design", *Soil Dynamics and Earthquake Engineering*, vol.22, 2002, p.765-772.
- [27] Tena-Colunga, A., Gómez-Soberón, L.A., "Torsional response of base-isolated structures due to asymmetries in the superstructure", *Engineering Structure*, vol.24 (12), 2002, p. 1587-1599.
- [28] Tyler, R.G., Robinson, W.H., " High-Strain tests on lead-rubber bearing for earthquake loadings", *Bull new Zealand Natl. Soc, Earthquake Engineering*, vol.7(2), 1984, p. 90-105.
- [29] Ryan, K.L., Kelly, J.M., Chopra, A.K., "Nonlinear model for lead–rubber bearings including axial-load effects", *Journal of Engineering Mechanics*, vol. 131(12), 2005: 1270–8.
- [30] Uang, C.M., "Establishing R or (Rw) and Cd factor building seismic provision", *Structural Engineering*, vol. 117(1), 1991, p. 19–28.
- [31] Wen, Y.K., Ellingwood, B.R., "The role of fragility assessment in consequence-based engineering", *Earthquake Spectra*, vol. 21(3), 2005: 861–77.